New Unsupported [100]-Oriented MoO₃ Catalysts

I. Preparation and Characterization

B. MINGOT,* N. FLOQUET,† O. BERTRAND,† M. TREILLEUX,‡ J. J. HEIZMANN,§
J. MASSARDIER,* AND M. ABON*,¹

**Institut de Recherches sur la Catalyse, Laboratoire Propre du CNRS, conventionné à l'Université Claude
Bernard Lyon I, 2 Avenue Albert Einstein, 69626 Villeurbanne Cédex, France; †Laboratoire de Recherches
sur la Réactivité des Solides, Faculté des Sciences de Mirande, B.P. 138, 21004 Dijon Cédex, France;
‡Département de Physique des Matériaux associé au CNRS, Université Claude Bernard, 43 Boulevard
du 11 Novembre 1918, 69622 Villeurbanne Cédex, France; and §Laboratoire de Métallurgie Structurale,
Faculté des Sciences, Ile de Saulcy, 57000 Metz, France*

In the general frame of the structure-sensitive character of the oxidation reactions of olefins and
alcohols on oxide catalysts, a new method of preparation of unsupported, [100]-oriented, MoO₃
catalysts is described. Diffraction techniques and SEM observations showed that the oxidation of
Mo sheets leads to MoO₃ oxide plates with a preferential [100] orientation of the crystallites, this
feature being most likely in relation with the special texture of the starting material. Moreover,
evidence is presented that MoO₃ (100) planes, which are believed to be active in the mild oxidation
of olefins, are actually truncated to (110), (120), or (130) surface planes. A structural model indi-
cates that such (1k0) planes should have a dual-site character and the consequences have been
discussed in relation with the mechanism of the mild oxidation of propene on MoO₃ catalysts.
© 1989 Academic Press, Inc.

I. INTRODUCTION

The catalytic properties of α-MoO₃ are
known to be structure-sensitive in the oxi-
dation reactions of olefins (*1–6*) and alco-
hols (*7–9, 11, 12*) and the reduction of nitric
oxide (*10*). However, there is still no gen-
eral agreement on the respective role of the
different exposed faces of MoO₃. In pro-
pene oxidation, Volta *et al.* (*1–5*) con-
cluded that mild oxidation to acrolein oc-
curs on the (100) faces whereas the (010)
faces are responsible for total oxidation.
Conversely, Brückman *et al.* (*6*) claimed
that the oxygen insertion step into allyl spe-
cies takes place on the (010) face. In metha-
nol oxidation, Tatibouet *et al.* (*7, 8*) ob-
served that formaldehyde is produced on
the (010) faces whereas, according to
Farneth *et al.* (*11, 12*), the (010) faces are
inactive in methanol conversion.

Clearly, further studies are needed on
well-characterized MoO₃ catalysts in order
to ascertain the respective roles of the (010)
and (100) faces and to specify the actual
structural and electronic features of these
surface planes.

Vapor-grown MoO₃ crystals are long,
thin platelets mainly exposing the basal
(010) face (which is the natural cleavage
plane of lamellar orthorhombic MoO₃).
Volta *et al.* (*1–5*) prepared graphite-sup-
ported MoO₃ catalysts from G–MoCl₅ in-
tercalated compounds with an improved
development of the side (100) faces as a
result of a support effect. However, struc-
tural or electronic characterization by most
surface-sensitive techniques is difficult on
these catalysts, owing to the small size of
the MoO₃ crystallites and also to the pres-
ence of the support.

In this paper we report on a new method
of preparation of unsupported α-MoO₃ by
complete oxidation of thin Mo foils. The

¹ To whom correspondence should be addressed.

preferential orientation and the morphology of the oxide sheets have been characterized by X-ray diffraction (XRD), transmission and scanning electron microscopy (TEM and SEM) and X-ray photoelectron spectroscopy (XPS). A forthcoming paper will be devoted to the activity of this new α-MoO₃ material as a catalyst for propene oxidation.

2. EXPERIMENTAL

2.1. Characterization of the Starting Material

The MoO₃ studied in this work was prepared from a thin polycrystalline foil of molybdenum (25 μm in thickness). Such Mo foils exhibit a fiber texture (see Fig. 1) with a preferential orientation Mo (100) $\langle 011 \rangle$ of the metal grains as determined by the pole figure technique (which is a complete, angular resolved, reflection XRD analysis); this particular orientation has also been shown by conventional reflection XRD. The diffraction pattern given by a Mo foil (Fig. 2a) displays only two peaks, (200) and (211), instead of those of the usual Mo pow-
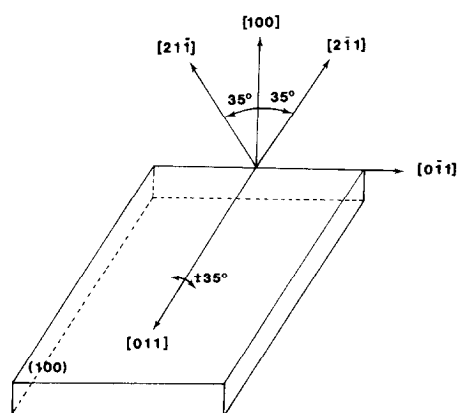

FIG. 1. Schematic representation of the preferential orientation of the Mo foil, as evidenced by the pole figure technique ($\langle 011 \rangle$ axis in the rolling direction).

der diffraction pattern (ASTM files) shown in Fig. 2b.

2.2. Oxidation of Mo Foils

The oxidation of the Mo foils has been performed in a quartz tube under a stream of pure oxygen (flow rate of 1.125 dm³ h⁻¹) at atmospheric pressure. The temperature
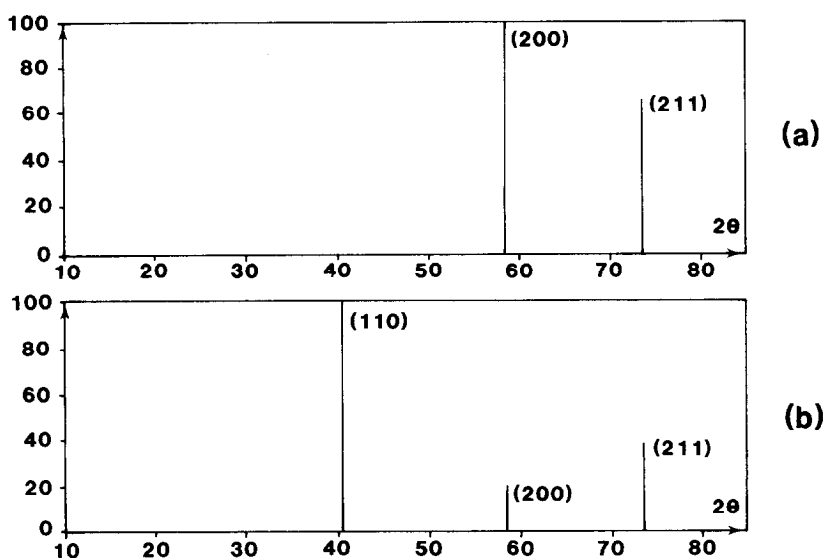

FIG. 2. Reflection XRD patterns of (a) Mo foil sample; (b) Mo powder (ASTM files) (note that in the b.c.c. crystal system, the structure factor is null if $(h + k + l)$ is odd).

TABLE 1

Characteristics of MoO_3 samples

Sample number	$T(K)^a$	$t(h)^b$	$\dfrac{I(200)^c}{\Sigma I(hkl)}$	$B(\mu m)^d$	$C(\mu m)^d$	B/C
1	773	260	98	0.15	0.60	0.25
2	809	190	91	0.25	1.10	0.23
3	843	65	63	0.5	2.0	0.25
4	863	48	44	0.8	3.0	0.27
5	893	24	40	1.0	4.5	0.22
6	923	12	47	1.5	6.0	0.25
7	953	6	40	3.0	12.0	0.25

^{a} T, temperature of oxidation.
^{b} t, time of oxidation.
^{c} $I(200)/(\Sigma I(hkl))$, as measured by XRD.
^{d} B and C, dimensions of MoO_3 crystallites, on outside surface.

of the Mo foil samples was first raised (heating rate, 4 K min^{-1}) to the chosen oxidation temperature which was then kept steady. The explored temperature range, from 773 to 953 K, was experimentally determined from thermogravimetry measurements. At lower temperatures (<773 K), the complete oxidation of molybdenum could not be reached even after very long oxidation times (>15 days). The higher temperature was chosen to limit a too high sublimation of the MoO_3 formed (MoO_3 melting point, 1068 K).

The seven prepared samples are listed in Table 1. The oxidized samples preserved their initial habit of foil, but they became friable and layered.

3. RESULTS

3.1. Reflection XRD

Two kinds of information have been sought for the oxidized Mo foils, namely a phase analysis performed on crushed samples and an analysis of the crystallite orientation performed on noncrushed oxide sheets laid flat on the diffractometer sample holder.

3.1.1. Phase analysis. Just after the oxidizing treatment, the platelets are all of the yellowish color typical of MoO_3 and after crushing the XRD pattern of a pure α-MoO_3 orthorhombic phase is obtained (Fig. 3a).

Some evolution with time of the color has been noticed: the platelets become darker and even gray, especially for samples prepared below about 873 K. These changes in color are reduced for samples kept light protected. It is known that the color of MoO_3 can change when exposed to light as a result of the photochromism phenomenon (13) leading to some reduction to the Mo^{5+} state. These changes in color can also be related to the presence of substoichiometric domains from MoO_3 to MoO_{3-x} ($x < 0.05$) as studied by Bursill (14) and Thöni et al. (15). The TEM images of some crystallites in Fig. 6a show contrasts of intensity which are related with such defects. There is no significant displacement of the ray position in the XRD analysis; the first suboxide characterized by a different XRD pattern is $Mo_{18}O_{52}$ (16).

3.1.2. Analysis of the crystallite orientation. The reflection pattern of the uncrushed oxidized Mo foils is very different from the α-MoO_3 powder pattern (see Figs. 3b and 3c with respect to Fig. 3a). For the samples oxidized at the lower temperatures, the XRD pattern is characterized by a nearly single (200) peak as shown in Fig. 3b. For samples oxidized at increasing temperatures up to 953 K, the XRD pattern is slightly modified: the intensity of the (200) peak remains the strongest while additional diffraction peaks, mainly (110) and (210), are growing in intensity (see Fig. 3c). In Table 1 we have summarized the change of the relative intensity of the (200) diffraction peak. These results support the preferential orientation of the [100] axis of MoO_3 crystallites formed at the lower temperatures. Further texture analysis with the pole figure technique has defined a complete fiber texture MoO_3 [100] axis, which leads to a schematic representation of the crystallites as represented in Fig. 4. Crystallites obtained at higher oxidation temperatures are slightly misoriented, up to 16° from this [100] MoO_3 axis. They are more or less tilted, allowing observation of the (210) and the (110) peaks (the angle between the (100)
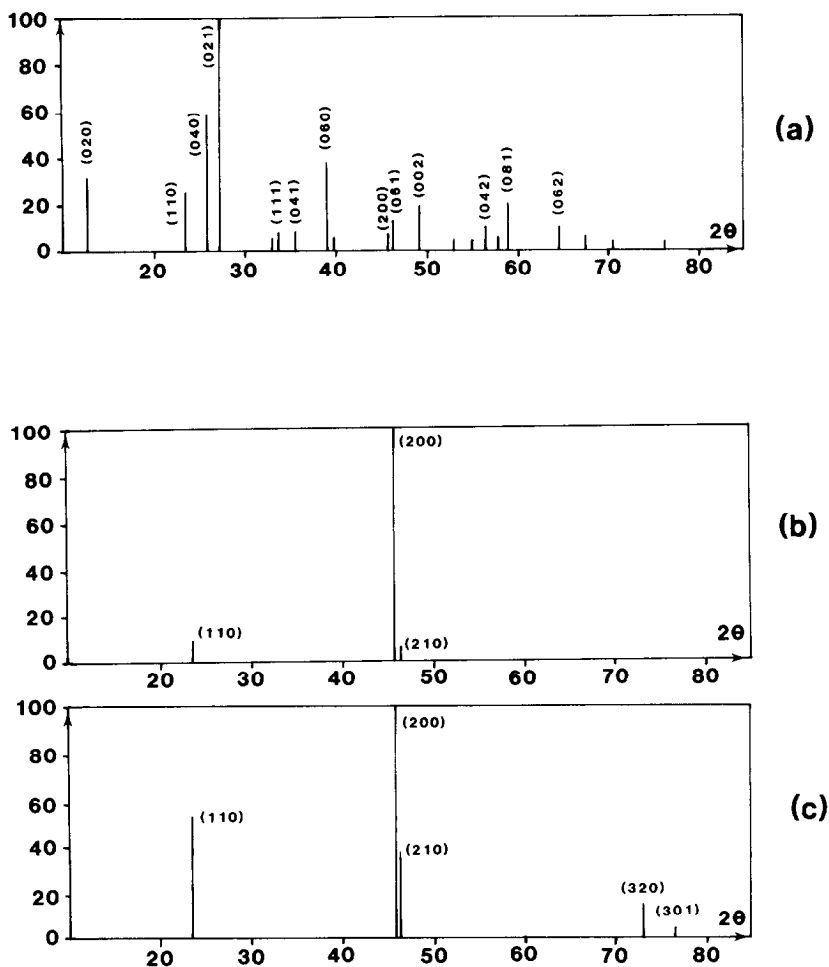
Fig. 3. Reflection XRD patterns of (a) sample 2 after crushing (note that, in the orthorhombic crystal system, the (100), (010), and (001) reflections are forbidden); (b) sample 2; (c) sample 6 (the sample definition is given in Table 1).

and the (210) planes is ~8° and between (100) and (110) ~16°.

Diffraction techniques do not give information on the shape of MoO_3 crystallites which have been depicted as parallelepipeds in Fig. 4. However, SEM observations have shown that crystallites exhibit a roof-like shape in the [100] direction, as described further on. We therefore indicate this actual shape on a magnified view of a crystallite.

3.2. X-Ray Photoelectron Spectroscopy

Whatever the temperature T of preparation of the MoO_3 platelets, the XPS analysis showed only peaks pertaining to Mo and O, with the exception of a small amount of carbon. Owing to charging shifts (16) resulting from the insulator character of MoO_3, the binding energies of XPS levels have been corrected after referencing to O (1s) at 530.3 eV (17, 18). The binding energy of the Mo 3d 5/2 and 3d 3/2 doublet, as shown in Fig. 5, corresponds to the 6+ oxidation state (18) for Mo, as expected for MoO_3. Although the gray color of the MoO_3 samples prepared at the lower temperatures suggests the presence of oxygen vacancies and hence also Mo^{5+} or Mo^{4+} ions, the present XPS observations show that, in the
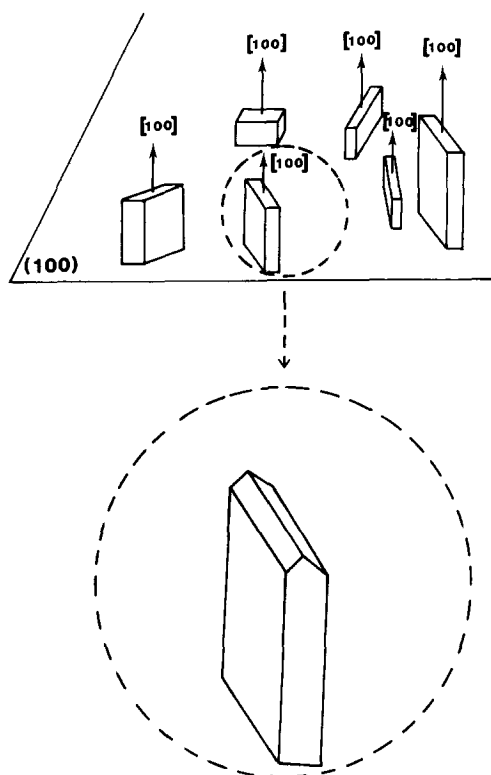
FIG. 4. Schematic representation of [100]-oriented MoO₃ crystallites in the oxidized Mo foils (with a magnified view showing the actual shape on the basis of SEM observations).

tals of the α-MoO$_3$ phase with size in the micrometer range (Fig. 6).

Microdiffraction patterns from several individual crystallites were obtained with the electron beam nearly normal to the oxidized foil. As shown in the inset of Fig. 6, the diffraction spots (001) and (020) correspond to a MoO$_3$ [100] zone axis pattern. The same type of microdiffraction pattern can be observed on nearly every crystallite.

Note that the (001) spots correspond to a forbidden reflection in the space group of the α-MoO$_3$ structure. Previous studies on the MoO$_3$ [010] zone axis have shown (100) and (001) forbidden reflections (19, 20) explained by the more or less curved nature of actual surfaces with the presence of steps of atomic height (19–21). The structure factor is then not null because the uppermost crystal unit cell is not complete.

Hence electron microdiffraction results confirm, at the single crystal level, the preferential orientation of the MoO$_3$ platelets already evidenced by XRD.

3.4. SEM Analysis

Oxidized foils are built up of a stacking of at least two strata of MoO$_3$ crystallites (each stratum is about 40 μm thick). Due to the layered morphology of the oxide, each foil sample of molybdenum usually generates two oxide plates. We thus call outside surfaces the original exterior surfaces and
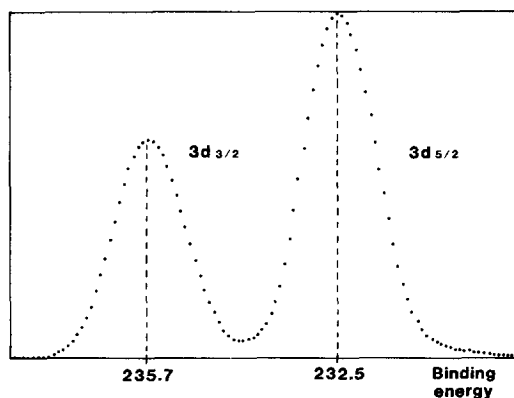
surface region, most Mo ions are in the 6+ oxidation state. However, the presence of less than a few percent of reduced ions (Mo^{5+} or Mo^{4+}) cannot be excluded, considering the sensitivity of the technique and the escape depth of the photoelectrons.

XPS analysis on crushed samples in order to investigate the oxidation state of the internal regions has not been performed because crushing fractures the crystallites and then generates many surface defects not representative of the normal surface state.

3.3. Transmission Electron Microscopy

The MoO$_3$ sample 2 (see Table 1), characterized by an intense (100) XRD peak, has been examined by TEM after a suitable thinning.

All observed crystallites are single crys-

FIG. 5. Typical electron XPS spectrum of the Mo 3d level given by the oxidized Mo foils (sample 4).

FIG. 6. TEM picture of MoO₃ crystallites (sample 2), including as an inset the electron microdiffraction pattern for the central crystallite (indicated by a white arrow).

inside surfaces the new surfaces created by the natural cleavage of the layered MoO₃ plates. SEM observations have been performed on the two types of surfaces (Figs. 7a and 7b) and also on cross sections in the whole thickness (Figs. 7c and 7d).

Figures 7a and 7b show that the MoO₃ crystallites look like rectangular platelets. These crystallites have their [100] axis normal to the surface as evidenced by diffraction techniques. Thus, the larger dimension C of the platelets corresponds to the [001] axis and the smaller dimension B to the [010] axis. In agreement with the schematic representation given in Fig. 4, there is no preferential orientation for [001] or [010] directions. A close examination of SEM pictures allowed us to measure average values of C and B on the outside surface of the MoO₃ plates and these observations, gathered in Table 1, clearly indicate that MoO₃ crystallites become larger and larger with

increasing oxidation temperatures. It is worth noting that the crystallites are much thicker than conventional vapor-grown MoO₃ crystals: $B/C \sim 0.25$ instead of about 0.03 as measured by Abou-Akar (22).

Inside surfaces look like outside surfaces, but MoO₃ crystallites are of smaller size and more numerous, as shown in Fig. 7b.

The evolution of the cross-section views with the oxidation temperature (Figs. 7c and 7d) is also very indicative of the changes with temperature in the crystallite morphology.

For a temperature of oxidation of 809 K (Fig. 7c), MoO₃ crystallites form parallel columns normal to the foil surface, that is, along the [100] axis as evidenced by diffraction techniques.

With increasing oxidation temperatures (see Fig. 7d), the columns break into larger and more individual crystallites growing
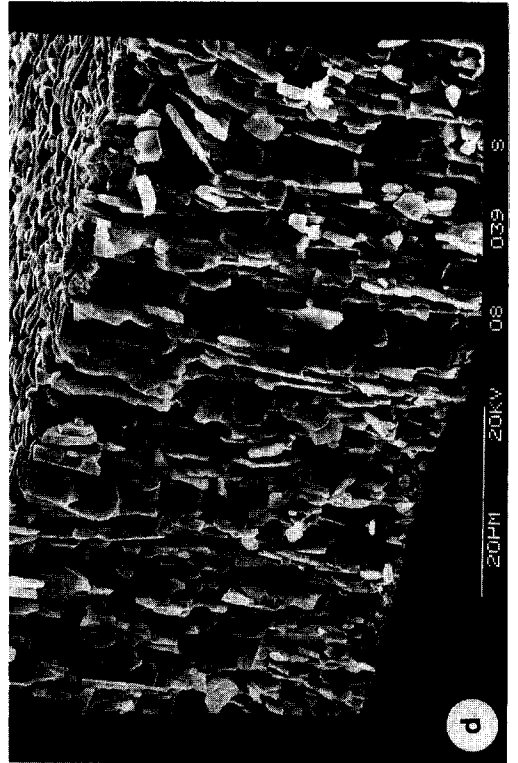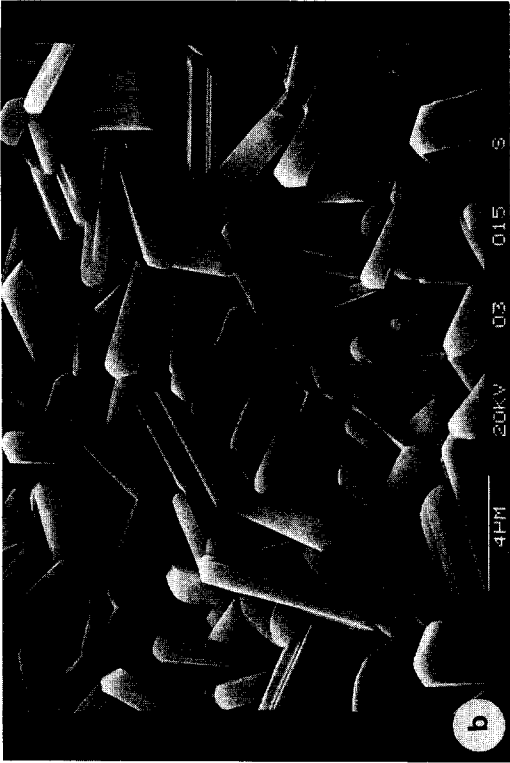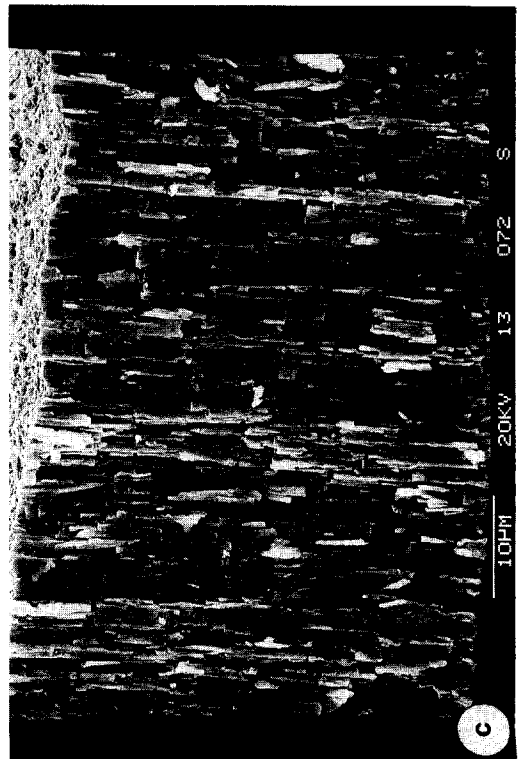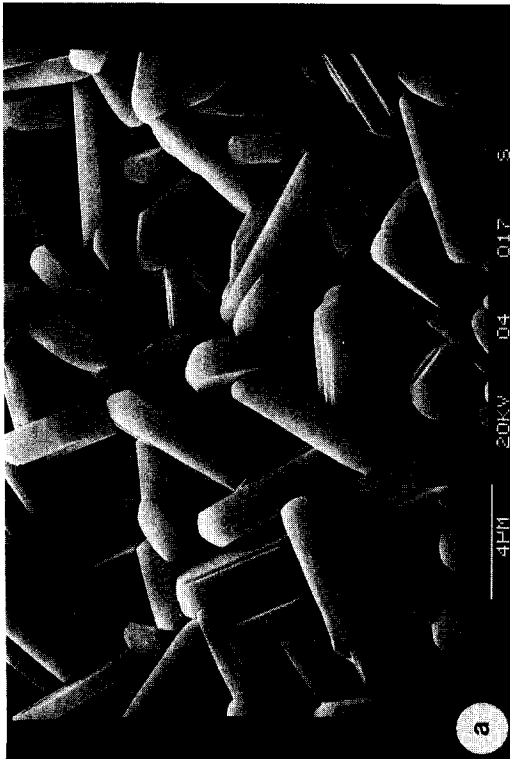
into each other. The MoO₃ [100] axis remains normal to the surface for most crystallites but some of them are more or less tilted, in agreement with the development of additional (210) and (110) peaks in XRD patterns.

The unusual thickness in the [010] direction of the MoO₃ crystallites and their [100] orientation normal to the oxidized foils allowed us to inspect closely their termination shape on the outside surfaces: instead of an expected flat (100) face, a roof-like shape has always been observed, with a central edge roughly parallel to the elongated [001] dimension, as shown in Fig. 8. This feature is especially apparent on large-size crystallites prepared at fairly high temperatures; the shape analysis is not accurate enough on small crystallites owing to a lack of resolution.

If MoO₃ crystallites do not terminate by (100) planes in the [100] direction, as suggested by these SEM observations, it would be of great interest to identify the actual surface planes. However, this determination cannot be precisely performed solely on the basis of SEM pictures such as those represented in Fig. 8, taken with incidence angles favoring perspective effects. Therefore several larger MoO₃ vapor-grown crystals have been examined by SEM along the [001] direction in order to look at the crystal profile normal to the [100] direction (see Fig. 9). Instead of the (100) faces at right angles with respect to (010) planes, truncations have always been observed and angle measurements show the presence of (1k0) planes such as (110), (120), and (130). The same identification emerges from optical goniometry measurements performed on fairly large MoO₃ crystals. It can therefore be reasonably assumed that the same (1k0) planes are present on the surface of the crystallites in the MoO₃ plates (Fig. 8), in

agreement with their roof-like shape with an edge [001] oriented.

4. DISCUSSION AND CONCLUSIONS

The results confirm a new method of preparation of the [100]-oriented unsupported α-MoO₃ catalyst. The oxidation of molybdenum foils in pure oxygen, in the range 773–953 K, leads to an orthorhombic MoO₃ phase. The oxidation front of the Mo foil, the growth axis of the MoO₃ crystallites, and their stacking are in the [100] MoO₃ direction which is a complete fiber axis of the oxide. MoO₃ crystallites are also characterized by a large thickness in the [010] direction, this feature thus favoring the development of the (1k0) faces. This special texture of the oxide may be induced by the texture of the starting material: the grains in the Mo foil also exhibit a preferential orientation most probably resulting from the rolling process of fabrication. However, an epitaxial relation does not seem obvious owing to the large differences in the crystal structure and lattice parameters of Mo and MoO₃.

As already discussed by Lattaud (23), the peculiar texture of an oxide prepared by oxidation in the bulk of a metal could be imposed by a preferential front for the oxidation reaction which exists to minimize the anisotropic mechanical stress caused by the lattice expansion on going from the metallic to the oxide state.

Systematic SEM observations mainly showed that the MoO₃ crystallites terminate, in the [100] direction, by surface planes such as (110), (120), or (130). We recall that up to now the side planes of MoO₃ crystallites were believed to be the (100), (001), (ī01), and (101) faces (4).

A first approach to the structure of these (1k0) surface planes can be made by consid-
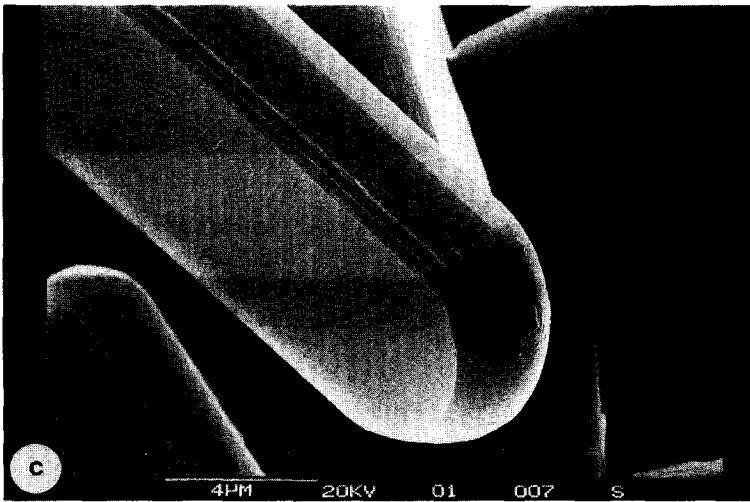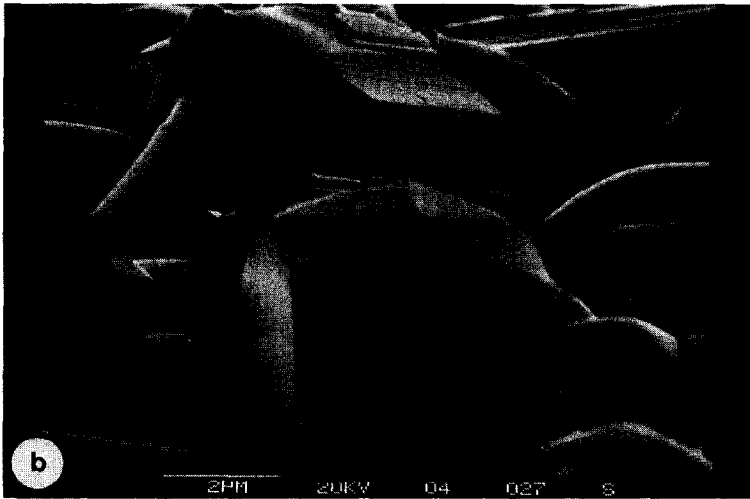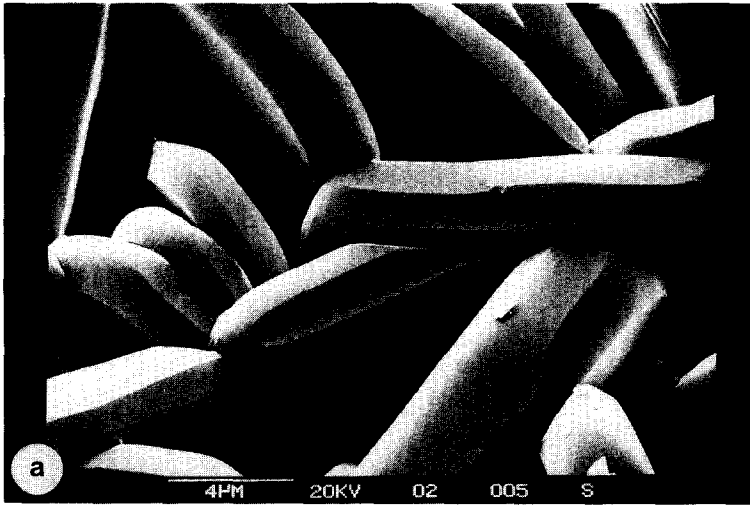
FIG. 8. Typical reflection SEM pictures showing the truncation of (100) faces with a [001]-oriented edge.
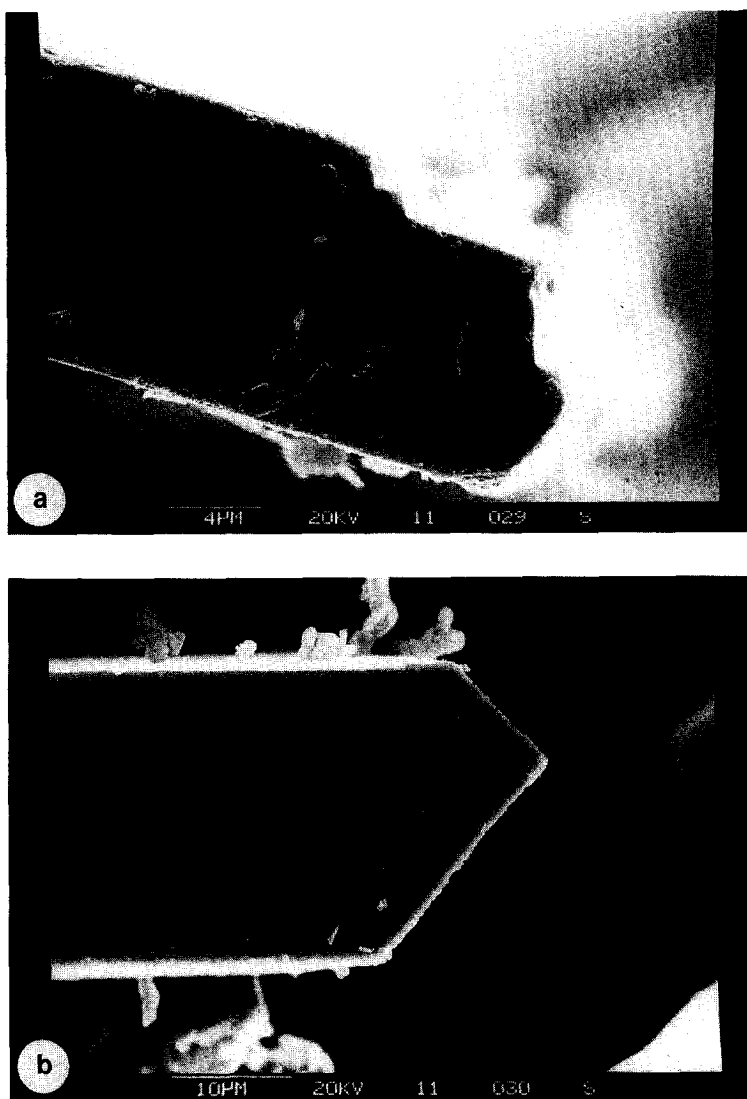
FIG. 9. Typical reflection SEM pictures of vapor-grown MoO_3 crystallites viewed along the [001] axis.

ering the known bulk structure of α-MoO_3 (24), which may be described as the stacking of two-level MoO_6 octahedra forming chains, linked together by van der Waals interactions. Figure 10 shows a projection on the (001) plane of this bulk structure limited by [010], [$\bar{1}$10], [$\bar{2}$10], and [$\bar{3}$10] directions. Figures 10a–10d thus give a profile view of the (100), (110), (120), and (130) planes which are all normal to the (001) plane of projection. The four planes (100),

(110), (120), and (130), as depicted in Fig. 10, are obviously closely similar and can be described as step-surfaces composed of (100) terraces and normal (010) steps.

This special geometry could induce a dual-site character which might be most important in the understanding of the mild oxidation mechanism of olefins, involving several important steps and several surface sites.

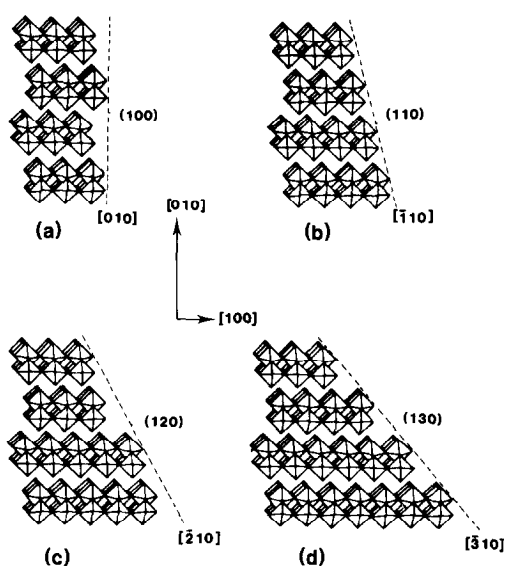Brückman *et al.* (6) proposed that pro-

FIG. 10. Projection of the MoO₃ bulk structure on the (001) plane cut to show the profile of (a) the (100) plane, (b) the (110) plane, (c) the (120) plane, and (d) the (130) plane. The angles between the (100) plane and the (110), (120), and (130) planes are, respectively, 15° 57′, 29° 45′, and 40° 37′. Lattice parameters: a, 3.96 Å; b, 13.86 Å; c, 3.69 Å.

pene activation occurs on the MoO₃ side faces, i.e., on (100), (001), and (101) faces, whereas the further step of lattice oxygen insertion is performed on the basal (010) face. Such a mechanism assumes a long lifetime of reactive allylic intermediates which moreover need to migrate on the surface from side faces toward (010) faces, by hopping across the MoO₃ sheets separated by van der Waals gaps.

Conversely a recent paper by Guerrero-Ruiz et al. (25) rather suggests that propene activation and the further oxygen insertion step occur on the same face (100).

These two proposals might be reconciled on the basis of the present study insofar as (1k0) faces are characterized by the presence in close proximity of

(i) Lewis acid–base sites, typical of the (100) face (1–5), where propene activation and dehydrogenation could occur;

(ii) oxo-groups Mo=O, typical of the

(010) face, which could be active in the oxygen insertion step (6).

Further work in progress on these [100]-oriented MoO₃ catalysts will include a study of their catalytic properties in propene oxidation. An attempt will also be made using physical surface sensitive techniques, to differentiate their geometric and electronic properties with respect to more conventional vapor-grown MoO₃ crystals mainly exhibiting (010) surface planes.

REFERENCES

1. Védrine, J. C., Coudurier, G., Forissier, M., and Volta, J. C., Catal. Today 1, 261 (1987).
2. Volta, J. C., and Portefaix, J. L., Appl. Catal. 18, 1 (1985).
3. Volta, J. C., and Tatibouet, J. M., J. Catal. 93, 467 (1985).
4. Volta, J. C., Forissier, M., Theobald, F., and Pham, T. P., Faraday Discuss. Chem. Soc. 72, 225 (1981).
5. Volta, J. C., Tatibouet, J. M., Phichitkul, C., and Germain, J. E., in "Proceedings, 8th International Congress on Catalysis, Berlin, 1984," Vol. 4, p. 451. Dechema, Frankfurt-am-Main.
6. Brückman, K., Garbowski, R., Haber, J., Mazurkiewics, A., Słoczýnski, J., and Wiltowski, T., J. Catal. 104, 71 (1987).
7. Tatibouet, J. M., and Germain, J. E., J. Catal. 72, 375 (1981).
8. Tatibouet, J. M., Germain, J. E., and Volta, J. C., J. Catal. 82, 240 (1983).
9. Baiker, A., and Gasser, D., Z. Phys. Chem. 149, 119 (1986).
10. Baiker, A., Dollenmeier, P., and Reller, A., J. Catal. 103, 394 (1987).
11. Machiels, C. J., Cheng, W. H., Chowdhry, U., Farneth, W. E., Hong, F., McCarron, E. M., and Sleight, A. W., Appl. Catal. 25, 249 (1986).
12. Farneth, W. E., Staley, R. H., and Sleight, A. W., J. Amer. Chem. Soc. 108, 2327 (1986).
13. Fleisch, T. H., and Mains, G. J., J. Chem. Phys. 76, 780 (1982).
14. Bursill, L. A., Proc. R. Soc. London A 311, 267 (1969).
15. Thöni, W., Gai, P. L., and Hirsch, P. B., Philos. Mag. 35, 781 (1977).
16. Bertrand, O., Floquet, N., and Jacquot, D., Surf. Sci. 164, 305 (1985).

17. Colton, R. J., Guzman, A. M., and Rabelais, J. W., *J. Appl. Phys.* **49,** 409 (1978).

18. Firment, L. E., and Ferretti, A., *Surf. Sci.* **129,** 155 (1983).

19. Dominguez-Esquivel, J. M., Guzman-Mandujano, O., and Garcia-Borquez, A., *J. Catal.* **103,** 200 (1987).

20. Dominguez-Esquivel, J. M., Fuentez-Mayado, S., Diaz-Guerrero, G., and Vasquez-Zavala, A., *Surf. Sci.* **175,** 701 (1986).

21. Nagakura, S., Nakamura, Y., and Suzuki, T., *Japan. J. Appl. Phys.* **21,** 449 (1982).

22. Abou-Akar, A., Thesis, Université Claude Bernard, Lyon I, 1987.

23. Lattaud, L., Thesis, Université de Dijon, 1984.

24. Kihlborg, L., *Ark. Kemi* **21,** 357 (1963).

25. Guerrero-Ruiz, A., Massardier, J., Duprez, D., Abon, M., and Volta, J. C., in "Proceedings, 9th International Congress on Catalysis, Calgary, 1988" (M. J. Phillips and M. Ternan, Eds.), p. 1601. Chemical Institute of Canada, Ottawa, 1988.